CDF/PUB/CDFR/PUBLIC/9625
Version 1.0
December 4, 2008

Setting Limits on GMSB Models in the $\gamma\gamma$ + $\not\!\!E_T$ Final State at CDF

CDF Collaboration

Abstract

We present the results of an optimized search for a gauge mediated supersymmetry breaking model with $\tilde{\chi}_1^0 \to \gamma\tilde{G}$ with low lifetimes in the $\gamma\gamma$+$\not\!\!E_T$ final state. We observed 1 event using 2.03 fb^{-1} of data collected by CDF II detector, which is consistent with the background estimate of 0.62 ± 0.29 events. We set cross section limits and mass limits as well as interpret our results for lifetimes up to 2 ns and find the exclusion region in the $\tilde{\chi}_1^0$ lifetime vs. mass plane with a mass reach of 138 GeV/c^2 at $\tau(\tilde{\chi}_1^0) = 0$ ns and cosmologically favored region.

1 Introduction

The Standard Model (SM) of elementary particles has been enormously successful, but it is incomplete. For theoretical reasons [1], and because of the '$ee\gamma\gamma$+missing transverse energy ($\not\!\!E_T$)' candidate event recorded by the CDF detector in RUN I [2], there is a compelling rationale to search in high energy collisions for the production of heavy new particles that decay producing the signature of $\gamma\gamma + \not\!\!E_T$.

An example of a theory that would produce these high energy photon events is gauge mediated supersymmetry breaking (GMSB) [1] with $\tilde{\chi}_1^0 \to \gamma\tilde{G}$ where the $\tilde{\chi}_1^0$ is the lightest neutralino and the next-to-lightest supersymmetric particle (NLSP) and $\tilde{G}$, a gravitino as the lightest supersymmetric particle (LSP). At the Tevatron gaugino pair-production dominates (See Figure 1) and the decays produce $\tilde{\chi}_1^0$'s in association with jets, with each $\tilde{\chi}_1^0$ decaying into a $\tilde{G}$, that gives rise to $\not\!\!E_T$, and a photon. Depending on how many of the two $\tilde{\chi}_1^0$'s decay inside the detector, due to their large decay length, the event has the signature $\gamma\gamma$+$\not\!\!E_T$ or γ+$\not\!\!E_T$ with one or more additional jets. Previous searches have been performed for such models in either $\gamma\gamma + \not\!\!E_T$ [3] or $\gamma + \not\!\!E_T$ [4] final state.

We focus on the optimization of the $\gamma\gamma$+$\not\!\!E_T$ search for GMSB models as this is more sensitive to low lifetimes, below nanoseconds, which is favored for large masses for cosmology regions [5]. For concreteness we use the Snowmass Slope constraint (SPS 8) [6] to quote results as a function of $\tilde{\chi}_1^0$ mass and lifetime. While GMSB provides model-dependent limits, by keeping our topological cuts to a minumum we keep a quasi model-independent, signature-based approach in our search, as well as providing a uesful benchmarks to compare our sensitivity with other searches at DØ [7] and LEP II [8].

We define our pre-selection sample by selecting events with two isolated, central ($|\eta| \lesssim 1.0$) photons with $E_T > 13$ GeV for the presence of significant $\not\!\!E_T$. All candidates are required to pass global event selection, photon ID, and non-collision background rejection requirements.

We perform a blind analysis in the sense that we blind the signal region and select the final event requirements based on the signal and background expectations alone. We optimize our predicted sensitivity using a simulation of our GMSB model and calculate, for each GMSB parameter point the lowest, expected 95% C.L. cross section limit as a function of the following event variables: $\not\!\!E_T$ *Significance*, H_T[1], and $\Delta\phi(\gamma_1, \gamma_2)$.

After all optimal cuts we open the box and observed one event, consistent with the expected 0.62±0.29 events. This event appears to be from the prompt collision background that is expected to dominate. Then we show the exclusion regions in neutralino mass and lifetime space for GMSB models.

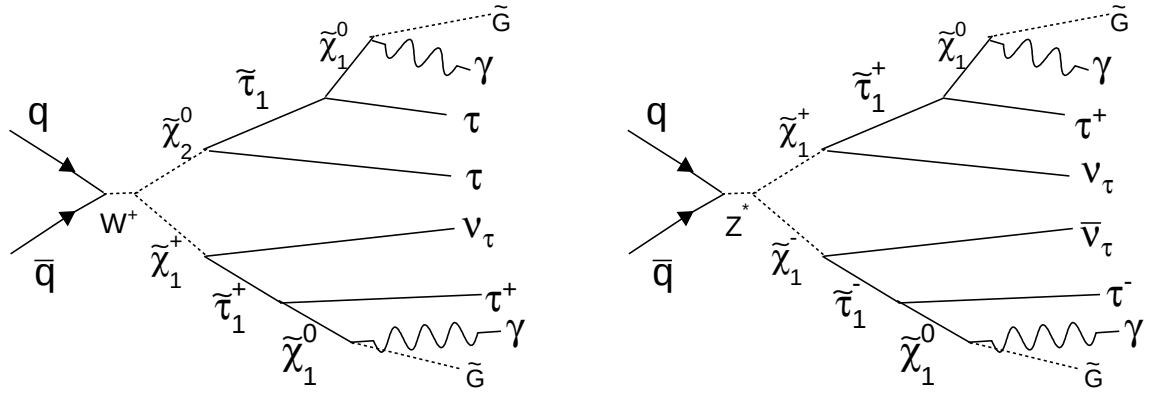

Figure 1: Feynman diagrams of the dominant tree production processes at the Tevatron for the GMSB model line we consider: $\tilde{\chi}_1^{\pm}\tilde{\chi}_2^0$ (45%) (a) and $\tilde{\chi}_1^{\pm}$ pair (b) production (25%). The τ's and second photons, if available, can be identified in the calorimeter as jets. Note that we only show one choice for the charge. The remaining processes are slepton (τ_1, e_R, μ_R) pair production.

2 Data Selection

The analysis is based on 2.034±1.22 fb^{-1} of data. The analysis selection begins with events that pass the CDF diphoton trigger. The trigger is 100% efficient for the final, offline selected γ and $\not\!\!E_T$.

Offline, we require both leading photons to be in the central, $|\eta| \leq 1.1$, pass the standard photon ID requirements and have $E_T^{\gamma} > 13$ GeV. In addition to the standard photon ID cuts we have added additional cuts to suppress PMT spikes and phoenix rejection cuts to remove events where an electron fakes a prompt photon.

We select events with $\gamma\gamma + \not\!\!E_T$ with at least one vertex of class 12 with $|z_{vx}| \leq$60 cm. The E_T of all calorimeter objects (individual towers, photons, electrons, and jets) are calculated with respect to the highest $\sum P_T$ vertex. Additional topology cuts are placed to reduce non-collision backgrounds, such as cosmic rays and beam halo effects.

Our pre-selection sample consists of 32,720 events left after all the quality, ID and cleanup cuts are applied. Table 1 gives a summary of the event reduction.

[1]Sum of E_T of all EM objects such as photons, jets with $E_T > 15$ GeV and $|\eta| < 2.4$ and $\not\!\!E_T$

Requirements	Signal sample (events passed)
Trigger, Goodrun, and Standard photon ID with $\|\eta\| < 1.1$ and $E_T > 13$ GeV	36,802
Electron faking photon rejection	33,899
PMT spike rejection	33,796
Vertex cuts	32,899
Beam Halo rejection	32,890
Cosmic rejection (EMTiming cut, after run 190851)	32,865
Cosmic rejection (Muon stub cut, before run 190851)	32,720
Total events passed	32,720

Table 1: Summary of $\gamma\gamma + \not\!\!E_T$ pre-sample selection requirements. Note we appy two different types of cosmic rejection cuts. EMTiming cuts are used to remove cosmic rays for data collected after run 190851 when the EMTiming system installed and, before events where there is a trackless muon stub in a cone of 30° around the direction of any of the two leading photons before then.

3 Backgrounds

There are five major sources of background for $\not\!\!E_T$ in $\gamma\gamma$ events: QCD events with fake $\not\!\!E_T$, electroweak events with real $\not\!\!E_T$, non-collision events (PMT spikes, cosmic ray or beam-halo events where one or more of the photons and $\not\!\!E_T$ are not related to the collision), wrong vertex events where there is no reconstructed vertex, and tri-Photon events with a lost photon that creates the fake $\not\!\!E_T$.

The final signal region for this analysis is defined by the subsample of pre-selection events that also passes a set of optimized final kinematic cuts. The methods for determining the background in the signal region are based on a combination of data and MC and allow for a large variety of final sets of cuts.

Standard Model QCD events, $\gamma\gamma$, $\gamma - jet \rightarrow \gamma\gamma_{fake}$, and $jet - jet \rightarrow \gamma_{fake}\gamma_{fake}$, are the dominent sources of events in the diphoton final state and a major background for $\gamma\gamma + \not\!\!E_T$. The energy fluctuations, which lead to considerable values of fake $\not\!\!E_T$, happen only in small fraction of cases, but the huge cross sections of these processes make them one of the largest backgrounds. However, we can significantly reduce the QCD background by selecting events based on $\not\!\!E_T$ $Significance$ using a new *Met Resolution Model*.

We use a sample of $Z/\gamma^* \rightarrow e^+e^-$ events to evaluate QCD background with fake $\not\!\!E_T$. To estimate the expected $\not\!\!E_T$ $Significance$ for the number of events above a given $\not\!\!E_T$ $Significance$ cut, we consider the jets and unclustered energy in the event and for each data event, we throw 10 pseudo-experiments to generate $\not\!\!E_T$ and calculate its significance according to the jets and underlying event configuration. Then we count the number of pseudo-experiments that pass our $\not\!\!E_T$ $Significance$ cut. This number divided by the number of pseudo-experiments gives us a prediction for the QCD background for a sample due to energy mis-measurements. In this way for any set of kinematic cuts for any sample we can predict the $\not\!\!E_T$ $Significance$ distribution.

Many electroweak processes with electrons in the final state have neutrinos, which gives intrinsic $\not\!\!E_T$ and can fake the $\gamma\gamma + \not\!\!E_T$ final state, having one common signature: $e\gamma \rightarrow \gamma_{cand}\gamma$, i.e. one photon is faked by electron and the other photon candidate can be either a real or fake photon.

To estimate the contribution from the electroweak backgrounds, we use the standard elec-

troweak MC samples and normalize to the production cross sections with a MC correlation factor. To normalize our results to data, we select $e\gamma + \not\!\!E_T$ events in data and MC. Then we take a ratio of $Data(e\gamma + \not\!\!E_T)/MC(e\gamma + \not\!\!E_T)$ to be a normalization factor in MC predictions for the $\gamma\gamma + \not\!\!E_T$ signature. While applying this normalization factor to predictions in the electron channels, we also take into account the Data-MC difference in the $e \to \gamma$ fake rate.

Non-Collision backgrounds to the $\gamma\gamma + \not\!\!E_T$ background come from PMT spikes, beam halo (B.H.) and cosmic rays (C.R.). PMT spikes are rare and have a distinct signature. The PMT asymmetry requirement removes them very efficiently. Therefore, we do not explicitly evaluate this background and take the number of remaining PMT spikes backgrounds events to be zero.

Beam halo events fake the $\gamma\gamma + \not\!\!E_T$ final state when high energy muons, produced in beam-beam pipe interactions, interact the calorimeter. we select a sample of $\gamma\gamma$ events after passing B.H. rejection cuts and use all selected B.H. events to create a template for various kinematic distributions. The template is scaled by the corresponding numbers of remaining B.H. events to obtain the contributions due to this background.

Cosmic ray events fake the $\gamma\gamma + \not\!\!E_T$ signature as the muon traverses the magnet, or by catastrophic interaction with the EM calorimeter. We use the muon system to suppress this type of background in data before run 190851, while we rely on the EMTiming system to remove the contamination due to cosmic ray after run 190851. We first determine the rate of $\gamma\gamma$-like cosmic events and the rejection power of a cut on the number of trackless muon stubs in "new" data after run 190851, and then extrapolate these results on the "old" data before run 190851.

To evaluate the number of the remaining cosmic events in date before run 190851, we use the observed number of cosmic events in the data with the EMTiming system and assume that the cosmics rate per bunch crossing is the same in both samples. This makes our final estimate for the number of the remaining cosmic ray events. Then, combining our predictions for "old" and "new" data, we predict the number of remaining cosmic ray events.

A source of QCD background that is unaccounted for by the *Met Model*, is di-photon events with a wrong choice of the primary interaction vertex. To obtain a prediction for this background contribution we use PYTHIA $\gamma\gamma$ events where the hard interaction does not produce a vertex, and the primary vertex is due to an overlapping Minimum Bias interaction. We first determine the fraction of such events in data. The fraction is used to normalize our MC template of "no vertex" $\gamma\gamma$ events to data.

There is a second class of QCD events whose contribution into the $\gamma\gamma + \not\!\!E_T$ signature is not estimated by the *Met Model*. These events are *tri-photon* events[2] with a lost photon that produces $\not\!\!E_T$. To estimate this background, we use a PYTHIA $\gamma\gamma$ sample with large statistics. We start by selecting reconstructed tri-photon candidate events ($E_T^{\gamma 1,2,3}$ >13 GeV) in both MC and data. This number gives us a MC-to-Data normalization factor. Then we select PYTHIA tri-photon events at the generator level, apply all of the analysis cuts to these events, and multiply the result by the the scale factor given above.

After estimating all the backgrounds, the expected $\not\!\!E_T$ $Significance$ distributions of all combined for the pre-sample are shown in Figure 2. This allows us to optimize by the number of events from the background estimation and the signal acceptance.

[2]One of the photon candidates can be a fake

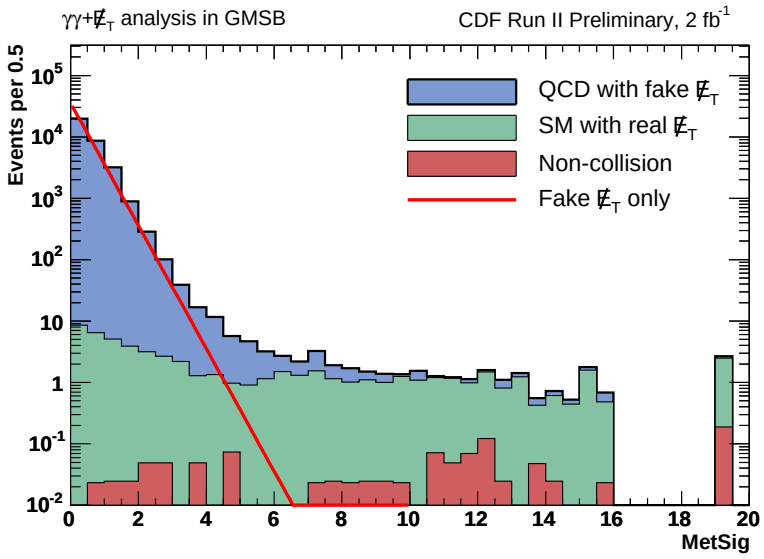

Figure 2: The background predictions for the pre-sample shows total predictions for all the backgrounds along with the perfect prediction of fake $\not\!\!E_T$ only.

4 GMSB Signal Monte Carlo

To estimate the acceptance for GMSB we use the PYTHIA event generator as well as a full detector simulation. For the purpose of this analysis we consider a GMSB model with the following parameters fixed on the minimal-GMSB Snowmass slope constraint (SPS 8) that is commonly used in Ref. [3, 8].

The breakdown of events after passing each of the selection cuts for an example GMSB point at $m(\tilde{\chi}_1^0) = 140$ GeV and $\tau(\tilde{\chi}_1^0) = 0$ ns near the limit, is shown in Table 2. For completeness we have included the results for the final event selection, determined in Section 5. We have ignored the muon stub cuts and different analysis for the early data for now as it produces only a $\sim 0.5\%$ difference.

Requirement	Events passed	$A_{\text{Signal MC}}$ (%) $m(\tilde{\chi}_1^0) = 140$ GeV and $\tau(\tilde{\chi}_1^0) = 0$ ns
Sample events	100000	100.00
Two EM Objects and $\lvert z_{vertex}\rvert < 60\ cm$	92010	92.0
Photon fiducial & Standard ID cuts	14190	14.2
Phoenix Rejection & PMT cuts	13785	13.8
Beam Halo and Cosmic Rejection cuts	13781	13.8
$\not\!\!E_T\ Significance$>3	10367	10.4
H_T>200 GeV	9802	9.8
$\Delta\phi(\gamma_1, \gamma_2)<\pi - 0.15$	9217	9.2

Table 2: Summary of the event reduction for a GMSB example point in the $\gamma\gamma$+$\not\!\!E_T$ final state. We have included the final, optimized cuts for completeness.

5 Results

Now that the background is estimated and the signal acceptance is available for a given set of cuts, an optimization procedure can be readily employed to find the optimal cuts before unblinding the signal region. We optimize for the following cuts: $\not\!\!E_T$ *Significance*, H_T, and $\Delta\phi(\gamma_1, \gamma_2)$.

As described in Section 3, $\not\!\!E_T$ *Significance* cut gets rid of most of the QCD background with fake $\not\!\!E_T$. H_T cut gives us a good separation in background and signal since in GMSB production heavy gaugino pari-prodcution dominates, which decays to high E_T, light final state particles via cascade decays. GMSB signal has lots of H_T compared to SM backgrounds, which is dominated by QCD and Electroweak backgrounds which do not have lots of high E_T objects. $\Delta\phi(\gamma_1, \gamma_2)$ cut gets rid of events where two photons are back to back since electroweak backgrounds with large H_T are typically a high E_T photon recoiling against $W \to e\nu$, which means the gauge boson decay is highly boosted. Also the high E_T diphoton with large H_T from QCD background are mostly back to back with fake $\not\!\!E_T$ or wrong vertex.

By estimating our sensitivity using the 95% C.L. expected cross section limits on GMSB models in the no-signal assumption, we find the optimal set of cuts before unblinding the signal region. We use the standard CDF cross section limit calculator [9] to calculate the limits, taking into account the predicted number of background events, the acceptance, the luminosity and their systematic uncertainties.

For each GMSB point there is a minimum expected cross section limit for a set of optimal cuts. As an illustration of the optimization, Figures 3-(a), (c), and (e) show the expected cross section limit as a function of a cut after keeping all other cuts fixed at the already optimized values. We decided to use a single set of cuts before we open the box based with the expectation that they will yield the largest expected exclusion region. We chose: $\not\!\!E_T$ *Significance*>3, $H_T>200$ GeV, $\Delta\phi(\gamma_1, \gamma_2)<\pi - 0.15$ rad. With thess cuts we predict 0.62 ± 0.29 background events with 0.39 ± 0.18 from SM electroweak with real $\not\!\!E_T$, 0.049 ± 0.050 from non-collision, and 0.10 ± 0.22 from QCD with fake $\not\!\!E_T$ listed in Table 3.

Figures 3-(b), (d), and (f) show the distributions of each optimization variable normalized to the number of expected events, after applying all optimized cuts. We compare the background distribution before unblinding the signal region and the expected signal in the signal region for an example GMSB point at $m(\tilde{\chi}_1^0) = 140$ GeV and $\tau(\tilde{\chi}_1^0) = 0$ ns. Taking into account the errors we expect an acceptance of $(9.21\pm1.66)\%$.

After all optimal cuts we open the box and observed one event, consistent with the expected 0.62 ± 0.29 events. Figure 4 shows the kinematic distributions for the background and signal expectations along with the data. There is no distribution that hints at an excess and the data appears to be well modeled by the background precdiction alone.

Background Source	Expected Rate±Stat±Sys
Electroweak	0.39±0.14±0.11
QCD	0.10±0.10±0.00
Non-Collision	0.049±0.042±0.028
Tri-Photon	0.00±0.180±0.035
Wrong Vertex	0.00±0.081±0.008
Total	0.62±0.26±0.12

Table 3: Summary of the background estimations after optimization.

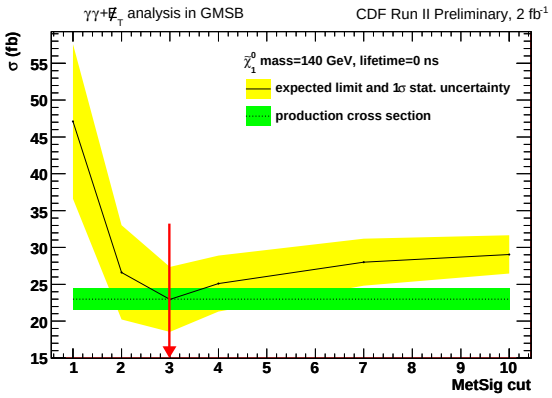

(a)

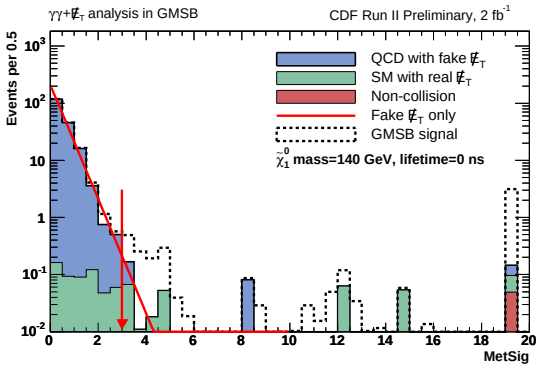

(b)

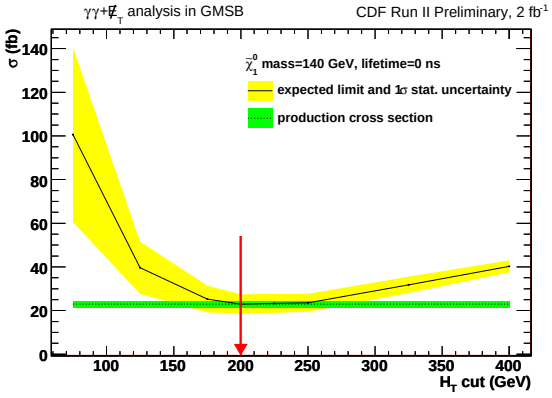

(c)

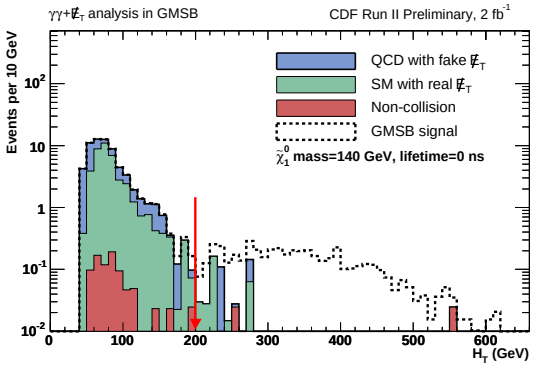

(d)

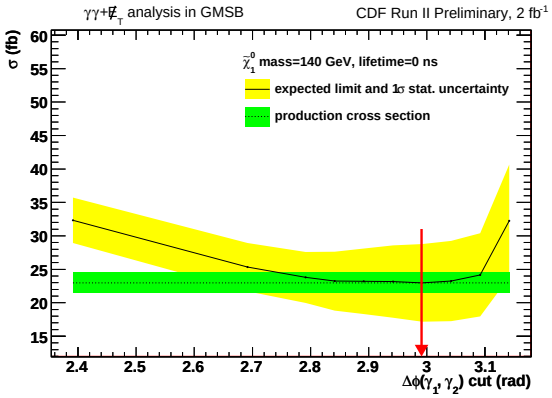

(e)

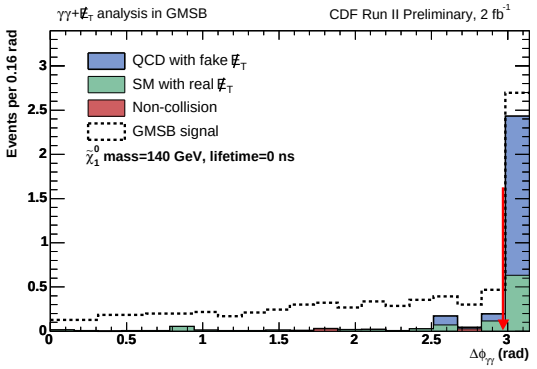

(f)

Figure 3: The expected 95% C.L. cross section limit as a function of the $\not\!\!E_T$ *Significance* (a), H_T (c), and $\Delta\phi(\gamma_1, \gamma_2)$ (e) requirement for a GMSB example point ($m(\tilde{\chi}_1^0) = 140$ GeV and $\tau(\tilde{\chi}_1^0) = 0$ ns). The optimal point is where the expected cross section is minimized. The N-1 predicted kinematic distributions after the optimized requirements are shown in Figure (b), (d), and (f).

Fig. 5 shows the predicted and observed cross section limits along with the NLO production cross section[3] as a function of $\tilde{\chi}_1^0$ lifetime at a mass of 140 GeV/c^2 and as a function of mass at a lifetime of 0 ns. The $\tilde{\chi}_1^0$ mass reach, based on the predicted (observed) number of events is 140 GeV/c^2 (138 GeV/c^2), at a lifetime of 0 and 1 ns. We do not consider lifetimes about 2 ns as most of the parameter space in high lifetimes there should be excluded by searches in single delayed photon analysis [5, 4]. Fig. 6 shows the 95% C.L. NLO exclusion region as a function of mass and lifetime of $\tilde{\chi}_1^0$ using the fixed choice of cuts from the optimization both for the predicted and observed number of background events. These limits extend the delayed photon results to both masses and lifetimes, at large masses, reaches well beyond those of DØ searches [7] and are currently the world's best.

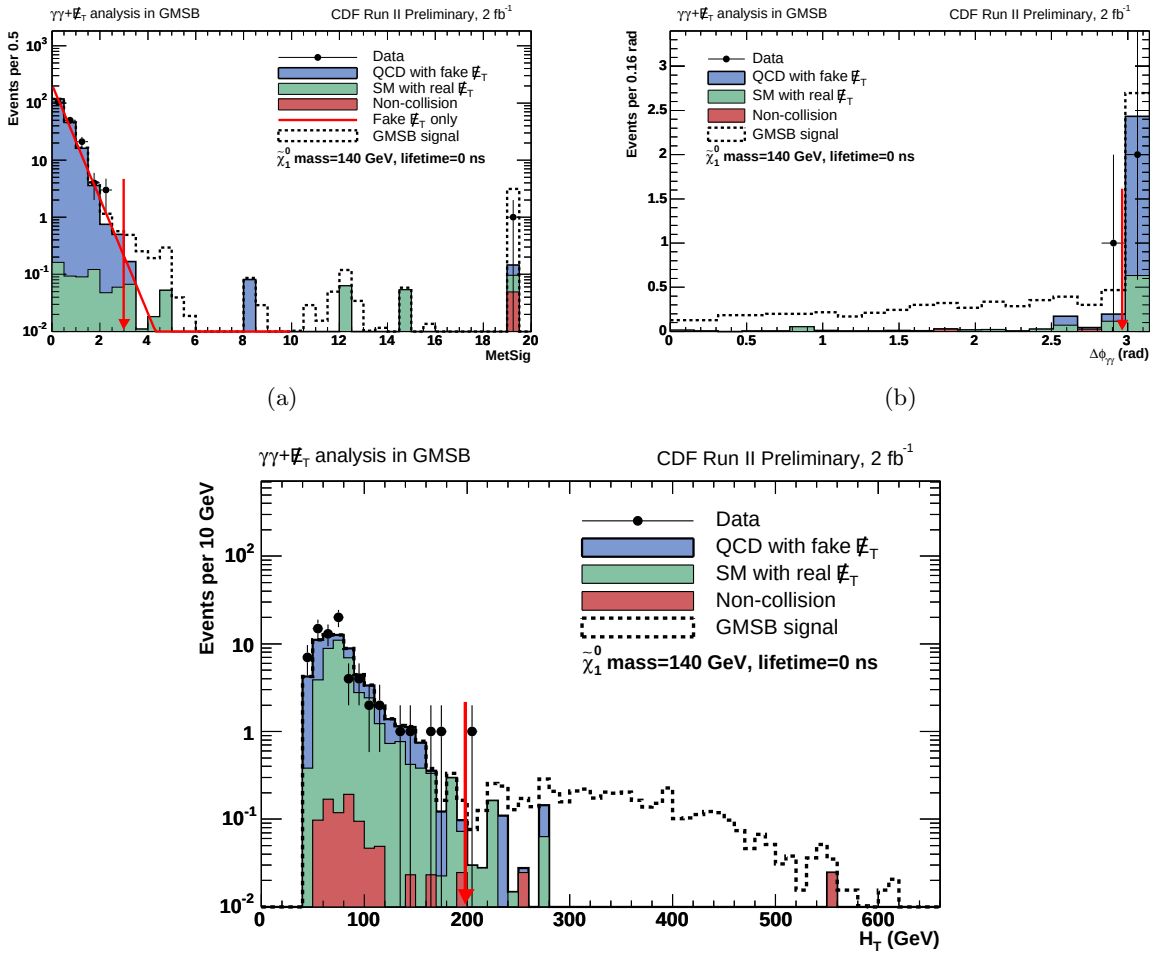

Figure 4: The same N-1 plots as Figure 3, but including the data. Each variable is plotted through the whole region while holding other variables at optimal cuts. There is no evidence for new physics.

[3]The production cross sections are calculated to leading-order using PYTHIA [10] with the NLO corrections using the K-factors as a function of $\tilde{\chi}_1^0$ masses for $\tilde{\chi}_1^{\pm}$ pair and $\tilde{\chi}_1^{\pm}\tilde{\chi}_2^0$ production taken from [11]

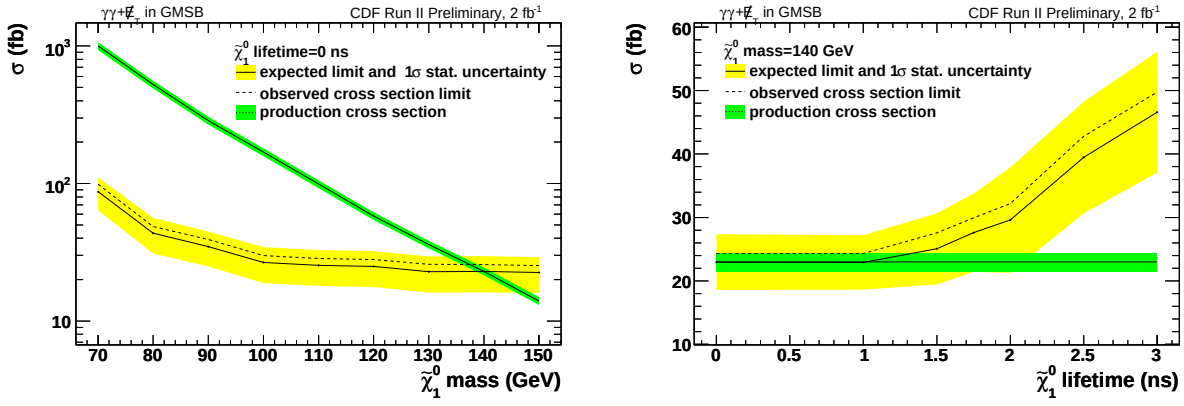

(a) (b)

Figure 5: The predicted and observed cross section limits as a function of the $\tilde{\chi}_1^0$ mass at a lifetime of 0 ns (a) and as a function of the $\tilde{\chi}_1^0$ lifetime at a mass of 140 GeV/c^2 (b).

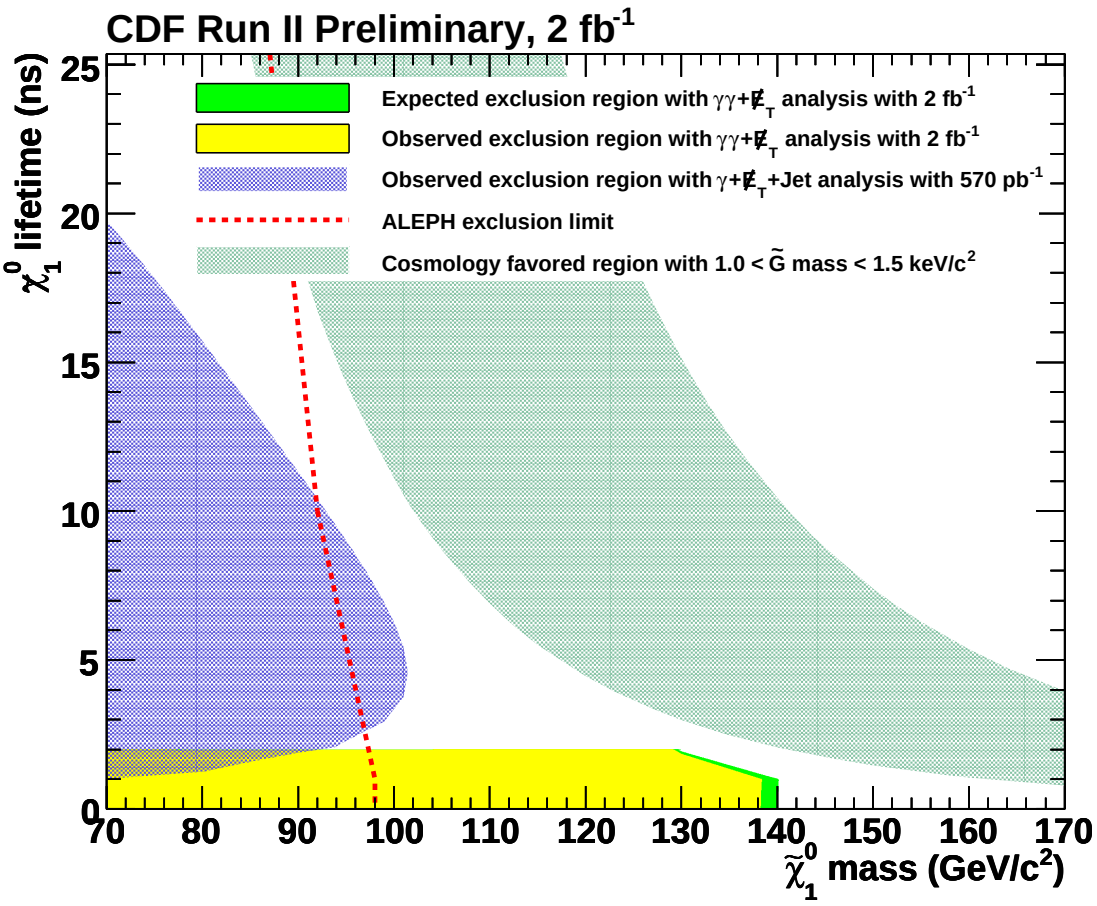

(a)

Figure 6: The predicted and observed exclusion region along with the limit from ALEPH/LEP [8] and delayed photon analysis [4]. We have a mass reach of 140 GeV/c^2 (predicted) and 138 GeV/c^2 (observed) at the lifetime up to 1 ns. The blue shaded band shows the parameter space where $1 \leq m_{\tilde{G}} \leq 1.5\ keV/c^2$, favored in cosmologically consistent models.

6 Conclusions and Prospects for the future

We have set limits on GMSB models using the $\gamma\gamma + \not\!\!E_T$ final state. Candidate events were selected based on the new $\not\!\!E_T$ resolution model technique, the EMTiming system and a full optimization procedure. We found 1 event using 2.03 fb^{-1} of data in run II which is consistent with the background estimate of 0.62±0.29 events from the Standard Model expectations. We showed exclusion regions and set limits on GMSB models with a $\tilde{\chi}_1^0$ mass reach of 138 GeV/c^2 at a $\tilde{\chi}_1^0$ lifetime of 0 ns. Our results extend the world sensitivity to these models.

To investigate the prospects of a search at higher luminosity we calculate the cross section limits assuming all backgrounds scale linearly with luminosity while their uncertainty fractions remain constant. Figure 7 shows the predicted exclusion region for a luminosity of 3 and 10 fb^{-1}.

For higher lifetimes (above ∼2 ns) the next generation delayed photon analysis will extend the sensitiviy and then will combine these results for completeness.

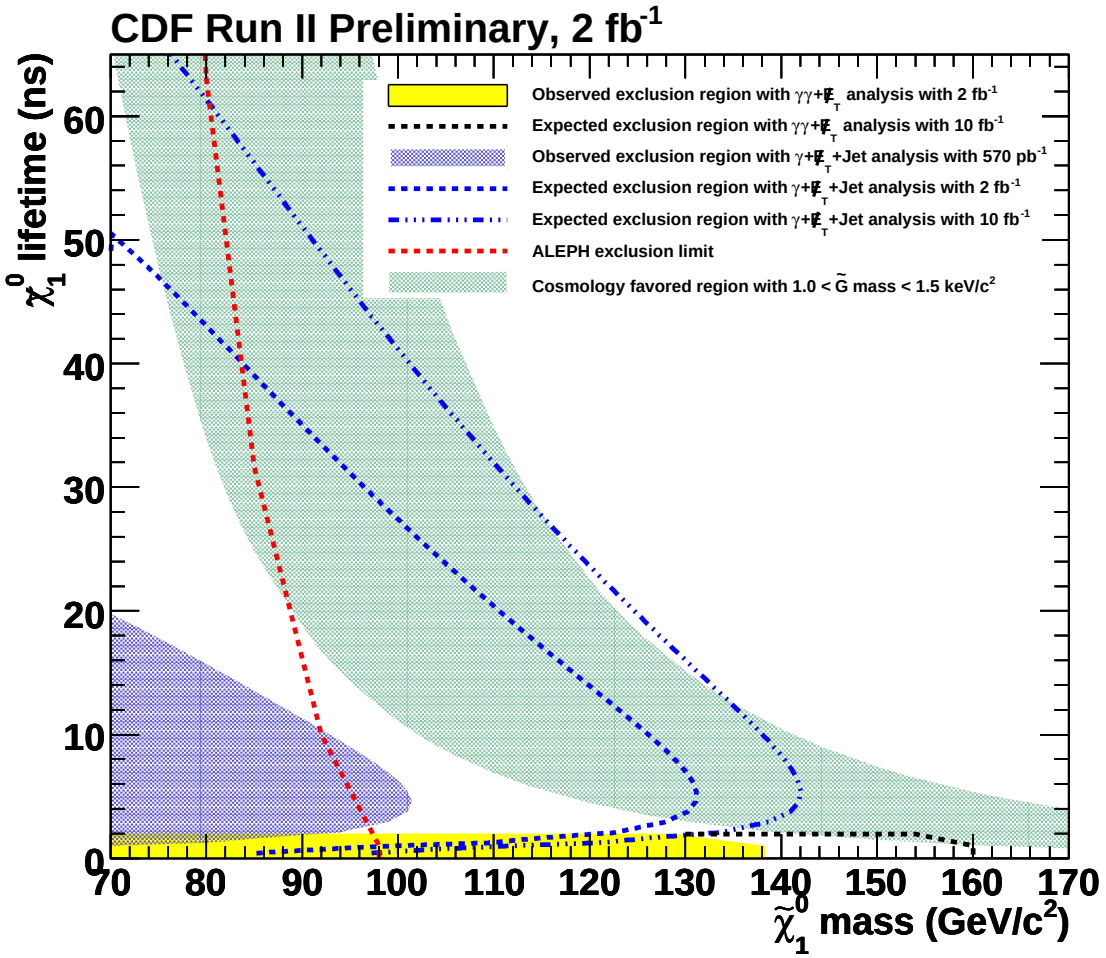

(a)

Figure 7: The black dashed line shows the prediction of the exclusion region limit after a scaling of the background prediction and the same fractional uncertainties for a luminosity of 10 fb^{-1}. The blue dashed lines show the prediction of the exclusion region limits from the delayed photon analysis for a luminosity of 2 fb^{-1} and 10 fb^{-1} respectively.

References

[1] See for example S. Ambrosanio, G. L. Kane, G. D. Kribs, S. P. Martin and S. Mrenna, Phys. Rev. D **54**, 5395 (1996) or C. H. Chen and J. F. Gunion, Phys. Rev. D **58**, 075005 (1998).

[2] CDF Collaboration, F. Abe *et al.*, Phys. Rev. Lett. **81**, 1791 (1998); Phys. Rev. D **59**, 092002 (1999).

[3] CDF Collaboration, D. Acosta *et. al.*, Phys. Rev. D **71**, 031104 (2005).

[4] CDF Collaboration, A. Abdulencia *et. al.*, Phys. Rev. Lett **99**, 121801 (2007); CDF Collaboration, T.Aaltonen *et. al.*, Phys. Rev. D **78**, 032015 (2008).

[5] P. Wagner and D. Toback, Phys. Rev. D **70**, 114032 (2004).

[6] B. C. Allanach *et. al.*, Eur. Phys. J. C**25**, 113 (2002).

[7] DØ Collaboration, V.M. Abazov *et. al.*, Phys. Lett. B **659**, 856 (2008).

[8] ALEPH Collaboration, A. Heister *et. al.*, Eur. Phys. J. C **25**, 339 (2002); A. Garcia-Bellido, Ph.D. thesis, Royal Holloway University of London (2002) (unpublished), arXiv:hep-ex/0212024.

[9] E. Boos, A. Vologdin, D. Toback and J. Gaspard, Phys. Rev. D **66**, 013011 (2002). J. Conway, CERN Yellow Book Report No. CERN 2000-005 (2000), p. 247.

[10] PYTHIA: T. Sjöstrand, L. Lönnblad and S. Mrenna, arXiv:hep-ph/0108264 (2001).

[11] W. Beenakker, *et al.*, Phys. Rev. Lett. **83**, 3780 (1999).